Regular Article

Investigation of Intracellular Delivery of NuBCP-9 by Conjugation with Oligoarginines Peptides in MDA-MB-231 Cells

Wei Wang,[a,b] Tadaharu Suga,[a,b] Masayori Hagimori,[a] Naotaka Kuroda,[b] Yuki Fuchigami,[a] and Shigeru Kawakami*,[a]

[a] Department of Pharmaceutical Informatics, Graduate School of Biomedical Sciences, Nagasaki University; 1–7–1 Sakamoto-machi, Nagasaki 852–8588, Japan: and [b] Department of Analytical Chemistry for Pharmaceutics, Graduate School of Biomedical Sciences, Nagasaki University; 1–14 Bunkyo-machi, Nagasaki 852–8521, Japan.

Oligoarginines (Rn) are becoming promising tools for the intracellular delivery of biologically active molecules. NuBCP-9, a peptide that induces apoptosis in B-cell lymphoma 2 (Bcl-2)-expressing cancer cells, has been reported to promote the uptake and non-specific cytotoxicity of R8, also called octaarginine. However, it is unknown whether a similar synergistic effect can be seen with other Rn. In this study, we conjugated NuBCP-9 with various Rn ($n=8, 10, 12, 14$) to investigate and compare their cellular uptake characteristics. In addition, their non-specific cytotoxicity and apoptosis-inducing abilities were evaluated. We found that NuBCP-9 conjugated with Rn enhanced cellular uptake mainly through clathrin-mediated endocytosis and macropinocytosis, and that the uptake pathways were not different from those used by unconjugated Rn. However, the cytotoxicity study showed that NuBCP-9-R12 and NuBCP-9-R14 conjugates enhanced non-specific cytotoxicity. We found that NuBCP-9-R10 conjugate had the highest uptake efficiency and induced correspondingly high levels of apoptosis, while resulting in a tolerable degree of non-specific toxicity.

Key words oligoarginine; NuBCP-9; endocytosis; B-cell lymphoma 2 (Bcl-2); intracellular delivery

Drug therapy is an indispensable part of clinical practices aimed at overcoming cancer, and can be applied independently or combined with other strategies. Any conventional therapeutic approach must mediate tumor cell death while minimizing side-effects. In general, traditional chemotherapeutic drugs lead to systemic toxicity resulting from non-specific distribution in the body. Small molecular drugs are therapeutic alternatives that exhibit more specificity in action. However, they are easily returned to circulation because of diffusion and excretion, and cannot be retained in tumors, resulting in poor pharmacokinetic profiles.[1] Pro-apoptotic peptides, such as acetyl-(KLAKLAK)2-NH$_2$ (KLA)[2] and the GO series of Mucin-1 inhibitors, are other promising alternatives to chemotherapy.[3] These could effectively and specifically induce cancer cell death.

Targeting B-cell lymphoma 2 (Bcl-2) is an efficient strategy for specifically inducing apoptosis in cancer cells. Many Bcl-2-targeted peptides have been reported in the literature.[4,5] Among them, NuBCP-9, an Nur77-derived peptide composed of 9 amino acids (FSRSLHSLL), exposes the BH3 domain of Bcl-2 and converts the anti-apoptotic Bcl-2 into an apoptosis inducer.[6] However, in contrast to the flexible membrane permeability of small molecular drugs, peptide drugs are membrane impermeable, restricting their uptake and activity. Therefore, additional vectors or components are required to ensure their passage through the cell membrane.

So far, cell penetrating peptides (CPPs)[7,8] and nanocarriers[9,10] have been studied as potential vectors for intracellular drug delivery. Compared to nanocarriers, CPPs require a simpler synthesis procedure and conjugation method, especially in the case of cargo peptides conjugated by amino acid linkers, which exhibit high cellular uptake efficiency.[11] Conjunction of cargo such as peptides to CPPs affects their cellular uptake.[12,13] Such changes greatly depend on the physicochemical properties of the cargo peptides. Relatively hydrophobic cargo peptides have demonstrated higher cellular uptake, but such enhancement has been shown to rely on the intrinsic uptake efficiency of the CPPs themselves.[12] In general, the uptake efficiency of oligoarginines (Rn), a kind of CPP, can be affected by the number of arginines comprising it.[14] Watkins et al. have demonstrated that the uptake efficiency of octaarginine (R8) can be significantly enhanced by conjugation with NuBCP-9.[15] Therefore, the uptake characteristics of Rn comprising varying numbers of arginine could be altered by conjugation with NuBCP-9. Furthermore, the non-specific cytotoxicity of R8 (unrelated to Bcl-2 expression) was shown to be magnified by NuBCP-9 conjugation.[15] Similarly, Jones et al. reported that scrambled peptide cargo significantly enhanced the non-specific cytotoxicity of human immunodeficiency virus trans-activating transcriptional activator protein (TAT), and polyarginines, although uptake was reduced.[16] Therefore, the uptake characteristics of Rn and NuBCP-9-Rn conjugates, as well as the non-specific cytotoxicity associated with their administration should be clarified. So far, little research has been performed on this subject.

In our study, we investigated the influence of NuBCP-9 conjugation on the uptake characteristics of various Rn that differed in the number of arginines comprising them. In addition, we compared the uptake pathways taken by various Rn and NuBCP-9-Rn conjugates in a Bcl-2 overexpressing cell line, MDA-MB-231 (human breast cancer cells).[17,18] We found that NuBCP-9-R12 and NuBCP-9-R14 conjugates resulted in severe non-specific cytotoxicity. Based on our results, NuBCP-9-R10 conjugate was concluded to be a good compound for inducing apoptosis through Bcl-2 in cancer cells while resulting in a tolerable degree of non-specific cytotoxicity.

* To whom correspondence should be addressed.   e-mail: skawakam@nagasaki-u.ac.jp

MATERIALS AND METHODS

Materials Chemicals used for peptide synthesis were purchased from Merck Millipore, Germany. Fluorescein-5-maleimide and 4-azidobenzoic acid (4-ABA) were purchased from TCI chemicals, Japan. Fetal bovine serum (FBS) was purchased from AusGene X, Australia, whereas other reagents for cell culture and chlorpromazine (CPZ) were purchased from Wako, Japan. Tris (2-carboxyethyl) phosphine hydrochloride (TCEP·HCl), genistein, and 5-(*N*-ethyl-*N*-isopropyl) amiloride (EIPA) were purchased from Sigma-Aldrich, Germany. LysoTracker Red and Hoechst 33342 were purchased from Invitrogen, U.S.A. Cell Counting Kit-8 (CCK-8) and lactate dehydrogenase (LDH) assay kits were purchased from Dojindo Molecular Technologies, Japan. The annexin V-fluorescein isothiocyanate (FITC) apoptosis assay kit was purchased from ImmunoChemistry, U.S.A. All other chemicals were reagent grade products obtained commercially.

Synthesis and Labelling of Peptides The peptides used in this study are listed in Table 1. They were synthesized by Fmoc (9-fluorenylmethyloxy-carbonyl) solid-phase peptide synthesis methods using Rink amide AM resin and Fmoc-L-amino acids as previously described.[19] Crude peptides were purified using reverse phase (RP)-HPLC. For fluorescent labelling, the peptides were reacted with TCEP·HCl and 4-ABA, incubated twice with fluorescein-5-maleimide in 4-(2-hydroxyethyl)-1-piperazineethanesulfonic acid (HEPES) buffer (50 mM, pH 7.0) for 2 h at room temperature in the dark. Then, the peptides were purified using RP-HPLC and lyophilized. The products were confirmed using HPLC and matrix assisted laser desorption/ionization-time of flight mass spectrometry (MALDI-TOF-MS; Bruker Daltonics Ultraflex, U.S.A.).

Cell Culture MDA-MB-231 cells (human breast cancer) were purchased from the European Collection of Authenticated Cell Cultures (ECACC) and were cultured in RPMI-1640 supplemented with 10% heat-inactivated FBS (Complete medium, CM), 100 U/mL penicillin, and 100 mg/mL streptomycin. Cells were maintained in a humidified 5% CO_2 incubator at 37°C.

Flow Cytometry $5.0 \times 10^4/cm^2$ MDA-MB-231 cells were seeded into 24-well plates (Violamo, Japan) and cultured for 24 h. The cells were incubated in culture medium containing peptides at 37°C for 30 min. After washing with phosphate-buffered saline (PBS), the cells were harvested and centrifuged at $300 \times g$ for 3 min at 4°C. After washing twice with ice-cold PBS supplemented with 20 units/mL of heparin, cells were re-suspended in PBS. The cells were analyzed using a flow cytometer (BD Biosciences, U.S.A.).

For investigating the uptake pathway, the cells were pre-incubated in culture medium containing the inhibitors (chlorpromazine, EIPA, and genistein at concentrations of 50, 100, and 200 μM, respectively) at 37°C for 30 min.[20] Then, the cells were incubated with peptides in the absence or presence of inhibitors at 37°C for 30 min. The remaining steps were the same as those described for flow cytometry above, following the 37°C-incubation step.

Confocal Laser Scanning Microscopy (CLSM) MDA-MB-231 cells were seeded onto 8-well chambered cover glasses (5.0×10^4 cells/cm²; Nunc Lab-Tek II, Thermo Scientific, U.S.A.) and incubated for 24 h. Then, the cells were incubated in culture medium containing the peptides at 37°C for 30 min. LysoTracker Red and Hoechst 33342 were used for staining late endosomes/lysosomes and nuclei, respectively. After washing, 1 μL of 0.4% trypan blue was added into the chamber using LSM 710 (Carl Zeiss, Germany) so that the intracellular distribution of the stained bodies could be observed.

To evaluate the effect of uptake inhibitors on the intracellular distribution of peptides, cells were pre-incubated with chlorpromazine (50 μM), genistein (200 μM) or EIPA (100 μM) at 37°C for 30 min, respectively. Then, fresh medium containing peptides was added in the absence or presence of inhibitors, and the cells were incubated at 37°C for 30 min. LysoTracker Red and Hoechst 33342 were used for staining, and the remaining steps were the same as those described above.

Cytotoxicity MDA-MB-231 cells (4.5×10^4 cells/cm²) were seeded into 96-well plates (Violamo, Japan) and cultured for 24 h. The cells were incubated in culture medium containing peptides for 2 h at 37°C. They were washed twice with PBS and continuously incubated in peptide-free culture medium for 22 h at 37°C. After incubation, CCK-8 was used to evaluate cytotoxicity.

LDH Assay MDA-MB-231 cells (4.5×10^4 cells/cm²) were seeded into 96-well plates and cultured for 24 h. Media change was given with fresh medium containing peptides, and the cells were incubated for 2 h at 37°C. After incubation, LDH assay kit was used to evaluate the release of LDH from the cells, which indicated the level of cellular cytotoxicity.

Apoptosis Detection MDA-MB-231 cells (4.5×10^4 cells/cm²) were seeded into 24-well plates (Violamo, Japan) and cultured for 24 h. Then, the cells were incubated in culture medium containing peptides for 2 h at 37°C. The cells were washed with PBS and continuously incubated in peptide-free culture medium for 22 h at 37°C. In the positive control group, cells were incubated in culture medium supplemented with 5 μM camptothecin for 4 h at 37°C. After trypsinization, the cells were collected and centrifuged at $300 \times g$ for 3 min. Following a PBS wash, cells were suspended in ice-cold binding buffer. Then, the cells were labeled with annexin-V-FITC and propidium iodide (PI) on ice for 10 min in the dark. The cell pellets were analyzed immediately by flow cytometry (BD

Table 1. Name and Sequence of Peptides Used in This Study

Unlabeled peptides	Sequence
R6	Ac-RRRRRRGC-NH₂
R8	Ac-RRRRRRRRGC-NH₂
R10	Ac-RRRRRRRRRRGC-NH₂
R12	Ac-RRRRRRRRRRRRGC-NH₂
R14	Ac-RRRRRRRRRRRRRRGC-NH₂
NuBCP-9	Ac-FSRSLHSLLGC-NH₂
NuBCP-9-R4	Ac-FSRSLHSLL-GGG-RRRRGC-NH₂
NuBCP-9-R6	Ac-FSRSLHSLL-GGG-RRRRRRGC-NH₂
NuBCP-9-R8	Ac-FSRSLHSLL-GGG-RRRRRRRRGC-NH₂
NuBCP-9-R10	Ac-FSRSLHSLL-GGG-RRRRRRRRRRGC-NH₂
NuBCP-9-R12	Ac-FSRSLHSLL-GGG-RRRRRRRRRRRRGC-NH₂
NuBCP-9-R14	Ac-FSRSLHSLL-GGG-RRRRRRRRRRRRRRGC-NH₂
FA-R8	Ac-FSRSLHSLA-GGG-RRRRRRRRGC-NH₂
AA-R8	Ac-ASRSLHSLA-GGG-RRRRRRRRGC-NH₂

All peptides consisted of L-form amino acids. For uptake investigation, fluorescein was conjugated with the cysteine (C) of peptides.

Biol. Pharm. Bull.

Biosciences, U.S.A.).

Statistical Analysis All comparisons of mean values were performed using ANOVA test. Unpaired *t*-test was utilized for two-group comparisons. Multiple comparisons among all groups were performed using two-way ANOVA with Bonferroni test. For comparisons between control and treatment groups, Dunnett test was used. Results yielding a *p* value less than 0.05 were considered statistically significant.

RESULTS

Cellular Uptake of Rn and NuBCP-9-Rn Conjugates The uptake level was analyzed by flow cytometry. After incubation with R8 or NuBCP-9-R8 conjugate for 30 min at 37°C, the uptake of NuBCP-9-R8 conjugate was found to be significantly higher than the uptake of R8 when the peptide dose was above 4μM (Fig. 1A). In previous studies, it has been reported that the uptake behavior of Rn differed depending on whether or not peptide concentration was above the threshold level.[21,22] Therefore, we selected 2 and 10μM for further experiments. Unconjugated NuBCP-9 showed negligible uptake at both doses. At 2μM, R12 showed the highest uptake level among Rn (Fig. 1B). NuBCP-9-R10 and NuBCP-9-R12 conjugates showed higher uptake levels than any other NuBCP-9-Rn conjugates. At 10μM (Fig. 1C), Rn showed an uptake efficiency similar to that seen at 2μM. On the contrary, the uptake of NuBCP-9-Rn conjugates was significantly enhanced at 10μM compared to the uptake of the same conjugates at 2μM. We found that NuBCP-9-R10 conjugate showed the highest uptake level at a concentration of 10μM.

Intracellular Distribution of Rn and NuBCP-9-Rn Conjugates CLSM was performed to determine cellular distribution of the administered peptides. At 2μM, Rn and NuBCP-9-Rn (*n*=8, 10, 12, 14) conjugates were internalized into punctate vesicles as shown in Fig. 1D. At 10μM, R8 was mainly located vesicular structures, as can be seen in Fig. 1E.

However, R10, R12, R14, and all NuBCP-9-Rn (*n*=6, 8, 10, 12, 14) conjugates were visualized as diffusely distributed in the cytoplasm. NuBCP-9-R8, and NuBCP-9-R10 conjugates showed significantly enhanced cytoplasmic labelling compared to NuBCP-9-R12 and NuBCP-9-R14 conjugates, and brighter staining of the nucleus by the peptides was observed in some cells (Fig. S1). The NuBCP-9-R10 conjugate exhibited the strongest cellular fluorescence signal. This was in agreement with the flow cytometry results depicted in Fig. 1C.

Investigation of the Uptake Pathway Taken by Rn and NuBCP-9-Rn Conjugates We examined the influence of three typical inhibitors of endocytosis pathways on the uptake behavior of Rn and NuBCP-9-Rn conjugates by flow cytometry. Chlorpromazine, genistein, and EIPA were selected as inhibitors against clathrin-mediated endocytosis, caveolae-mediated endocytosis, and macropinocytosis, respectively.[20] In the presence of chlorpromazine or EIPA, the uptake of R8 and NuBCP-9-R8 conjugate was significantly suppressed in MDA-MB-231 at both peptide concentrations (Figs. 2A, B). Similar results were obtained with Rn and NuBCP-9-Rn conjugates (*n*=10, 12, 14) (Fig. S2). Co-incubation with genistein did not inhibit the uptake of peptides.

Intracellular Distribution of Rn and NuBCP-9-Rn Conjugates in the Presence of Uptake Inhibitors At concentrations of 2 or 10μM (Figs. 2C, D, Fig. S3), when compared with control group (no inhibitors), the uptake level of peptides was suppressed under chlorpromazine or EIPA treatment. In addition, the subcellular distribution was changed, with staining in the nucleolus or diffuse cytoplasmic staining becoming much dimmer than that seen in the control group. Cells co-incubated with peptides and genistein showed no changes in cellular distribution of the peptides or fluorescence staining intensity when compared with the control group cells.

Investigation of Uptake Mechanism of NuBCP-9-R8 Conjugate by Amino Acid Replacement of NuBCP-9 To investigate the presence of a hydrophobicity switch with
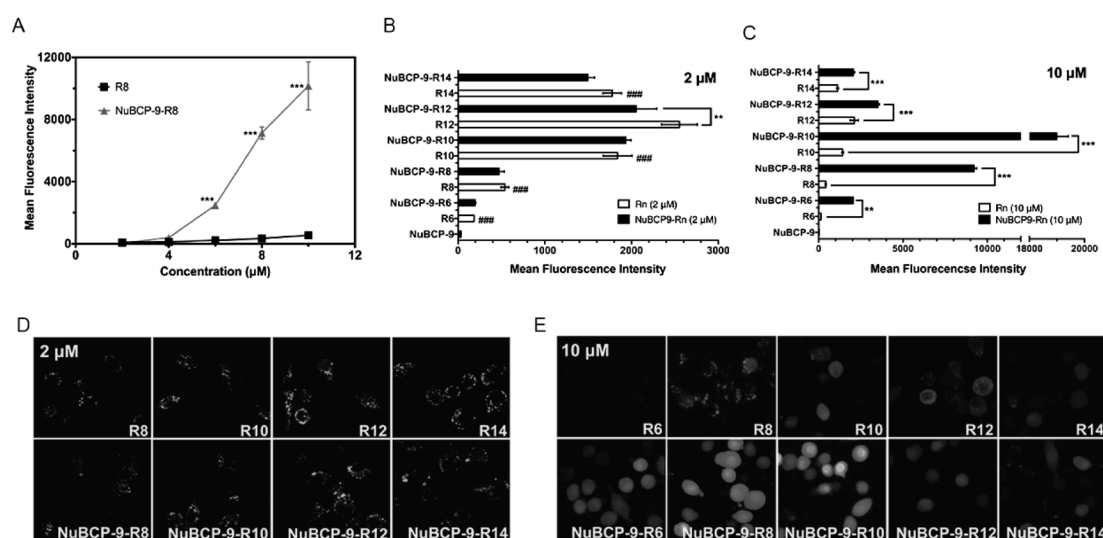

Fig. 1. Internalization and Subcellular Distribution of Rn and NuBCP-9-Rn Conjugates

MDA-MB-231 cells were incubated with fluorescein labeled peptides for 30 min at 37°C. Fluorescein-labeled peptides refer to (A) 2–10 μM R8 or NuBCP-9-R8 conjugate (B) 2 μM or (C) 10 μM Rn or NuBCP-9-Rn (*n*=0, 6, 8, 10, 12, 14) conjugates, respectively. The uptake level was quantified by flow cytometry. Error value represents the mean±S.D. from triplicate experiments. 10000 counts were taken for each sample. (ANOVA, Bonferroni test, *Significant difference between Rn and NuBCP-9-Rn conjugates, **$p<0.01$, ***$p<0.001$, #Significant difference between R12 and each treatment with Rn, ###$p<0.001$). MDA-MB-231 cells were incubated with (D) 2 μM or (E) 10 μM fluorescein-labeled Rn and NuBCP-9-Rn (*n*=6, 8, 10, 12, 14) conjugates for 30 min at 37°C and then analyzed by confocal microscopy. (The color images with Lysotracker Red and Hoechst 33342 staining are shown in Fig. S1.)
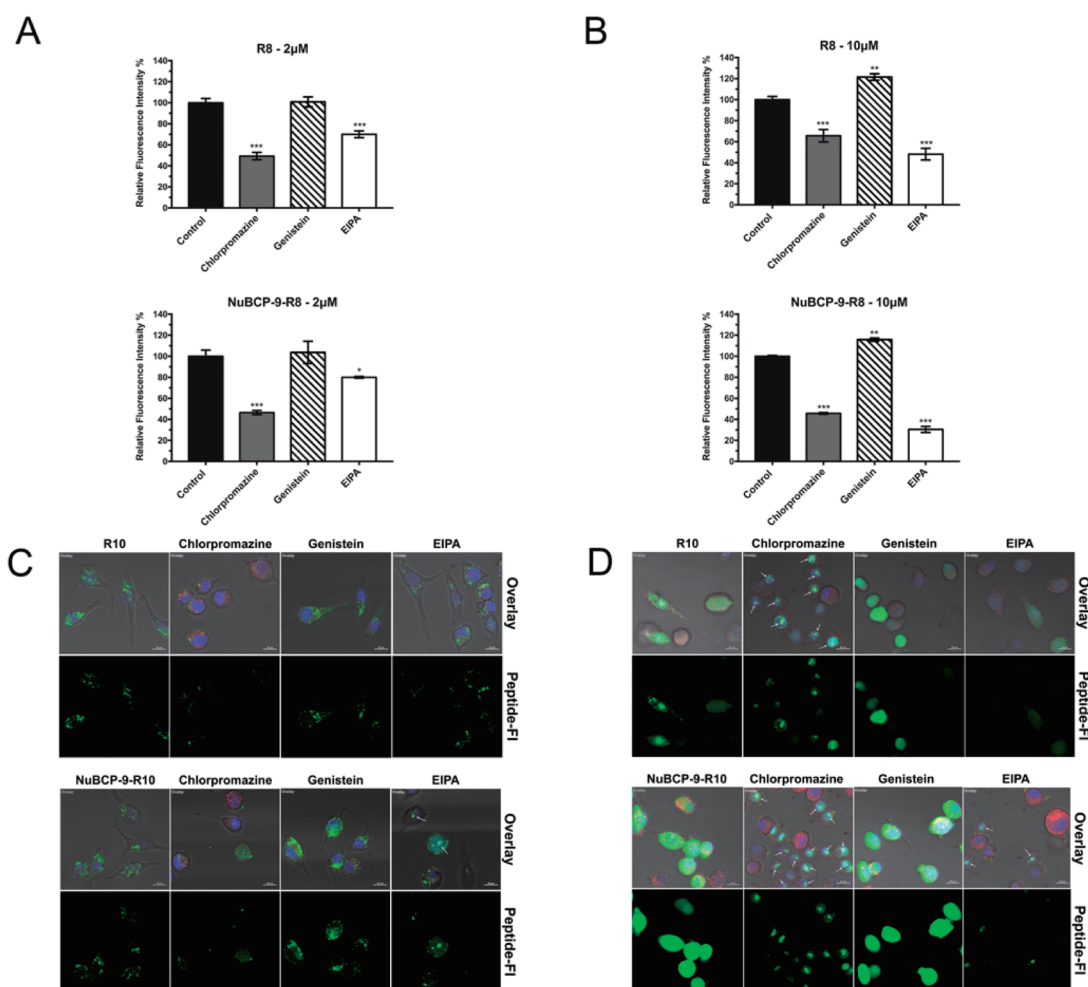
Fig. 2. Mechanism of Cellular Uptake of Rn and NuBCP-9-Rn Conjugates

MDA-MB-231 cells were incubated for 30 min with (A) 2 μM or (B) 10 μM R8 or NuBCP-9-R8 conjugate in the absence or presence of 50 μM CPZ, 200 μM genistein, or 100 μM EIPA, respectively. Uptake of peptides was quantified by flow cytometry. The results are expressed as a percent of the fluorescence measured in the absence of inhibitors. Each value represents the mean±S.D. from triplicate experiments. 10000 counts were taken for each sample. (ANOVA, Dunnett test, *$p < 0.05$, **$p < 0.01$, ***$p < 0.001$) (the figures for other peptides are given in Fig. S2). The cellular distribution of (C) 2 μM or (D) 10 μM of R10 or NuBCP-9-R10 conjugate (green) in the absence or presence of uptake inhibitors under same conditions were also analyzed by confocal microscopy. Lysotracker Red (red) and Hoechst 33342 (blue) were added in the medium for lysosomal and nuclear staining, respectively. Arrows indicate peptide labelling of the nucleolus. (The images for other peptides are given in Fig. S3.) Scale bars: 10 μm.

respect to the uptake of NuBCP-9-R8 conjugate in MDA-MB-231 cells, we synthesized NuBCP-9-R8-derived conjugates (FA-R8 and AA-R8) with differing hydrophobicities resulting from a molecular change at their distal ends (Table 1). FA-R8 replaced leucine with alanine at C-terminus of NuBCP-9-R8. At 10 μM, there was an approximately 300% decrease in the uptake of FA-R8 relative to NuBCP-9-R8. AA-R8 replaced phenylalanine with alanine at N-terminus of FA-R8. There was an approximately 700% decrease in the uptake of this modified conjugate at 10 μM relative to FA-R8 (Fig. 3). The NuBCP-9-R8-derived conjugate with low hydrophobicity at both its distal positions, AA-R8, in fact had an uptake level similar to that of unconjugated R8.

Cellular Cytotoxicity of NuBCP-9-Rn Conjugates and Rn The cytotoxicity of NuBCP-9-Rn ($n=0, 4, 6, 8, 10, 12, 14$) conjugates at concentrations up to 15 μM is shown in Fig. 4A. The derived IC_{50} values are summarized in Table 2. Treatment with NuBCP-9 (without Rn conjugation), NuBCP-9-R4 or NuBCP-9-R6 conjugates lead little cytotoxicity up to 15 μM in MDA-MB-231. NuBCP-9-Rn ($n=8, 10, 12, 14$) conjugates showed concentration-dependent cytotoxicity. As the length of
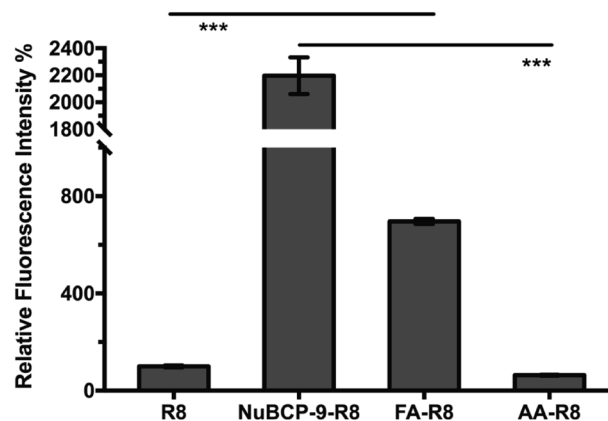

Fig. 3. Uptake Efficiency of Conjugates with Modified Hydrophobicity

Cells were incubated with 10 μM fluorescein-labeled R8, NuBCP-9-R8 conjugate, FA-R8 conjugate, and AA-R8 conjugate for 30 min at 37°C. The uptake level was quantified by flow cytometry. Each value represents the mean±S.D. from triplicate experiments. (ANOVA, Bonferroni test, ***$p < 0.001$.) 10000 counts were measured for each sample.
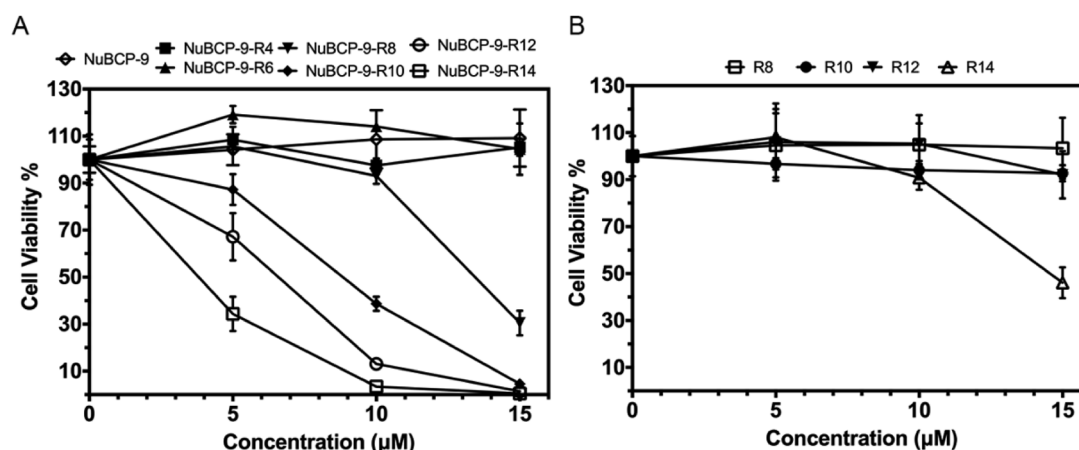
Fig. 4. Cytotoxicity of Rn and NuBCP-9-Rn Conjugates in MDA-MB-231 Cells

(A) Viability of MDA-MB-231 cells following a 2h incubation with 0–15 μM unlabeled NuBCP-9-Rn ($n=0, 4, 6, 8, 10, 12, 14$) conjugates and then a 22h incubation in the absence of peptides. Each value represents the mean±S.D. from triplicate experiments. (B) Viability of MDA-MB-231 cells following a 2h incubation with 0–15 μM unlabeled Rn ($n=8, 10, 12, 14$) and then a 22h incubation in the absence of peptides. Each value represents the mean±S.D. from triplicate experiments.

Table 2. IC_{50} of Rn and NuBCP-9-Rn Conjugates ($n=8, 10, 12, 14$) in MDA-MB-231 Cells

Number of arginine (n)	IC_{50} (μM)	
	Rn	NuBCP-9-Rn
8	N.D.	13.51
10	N.D.	8.31
12	N.D.	6.08
14	14.58	4.10

N.D., not done.

Rn increased, the IC_{50} of NuBCP-9-Rn conjugates decreased. When the cells were treated with unconjugated Rn, there was little cytotoxicity with R8, R10, and R12 at concentrations of up to 15 μM. R14 showed low toxicity at 10 μM, but only 46.08±6.58% ($n=3$) cells were viable at 15 μM (Fig. 4B).

Non-specific Cytotoxicity of NuBCP-9-Rn Conjugates and Rn The cytotoxicity of NuBCP-9-Rn conjugates did not correlate well with their uptake efficiency as determined by flow cytometry. Rn induces non-specific cytotoxicity at high doses owing to its strong electrostatic interaction with the cell membrane.[14,23] Therefore, we considered the possibility that membrane integrity may be disturbed by short-time incubation of cells with the peptides. We measured cellular LDH levels after treatment with peptides to estimate membrane disruption. As can be seen in Fig. 5, following conjugation with NuBCP-9, LDH release increased with increasing length of Rn. NuBCP-9-R12 and NuBCP-9-R14 conjugates induced 43.97±0.65 and 76.09±1.59% ($n=3$) LDH release at 10 μM, respectively. While unconjugated Rn ($n=8, 10, 12$) caused negligible membrane disruption in MDA-MB-231 cells at 10 μM, the most toxic peptide, R14, disturbed membrane integrity of 5.94±0.32% cells, which is still significantly less membrane damage than that caused by the conjugates.

Induction of Apoptosis in MDA-MB-231 Cells Following Incubation with Peptides The mechanism of cell death caused by NuBCP-9 has been reported as pro-apoptosis, occurring through exposing BH3 domain of Bcl-2.[6] In our study, we detected the level of apoptosis induced by 10 μM of NuBCP-9-R8 conjugate, NuBCP-9-R10 conjugate, and
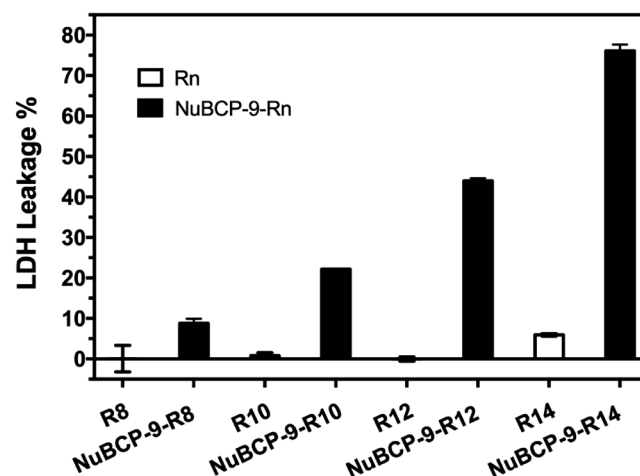

Fig. 5. Membrane Integrity of MDA-MB-231 Cells Following a 2h Incubation with 10 μM Unlabeled Rn and NuBCP-9-Rn ($n=8, 10, 12, 14$) Conjugates

Each value represents the mean±S.D. from triplicate experiments.

R10. Following staining with annexin V-FITC and PI, MDA-MB-231 cells were analyzed by flow cytometry. From Fig. 6, it can be seen that R10-treated cells and the negative control group showed similar levels of apoptosis. NuBCP-9-R10 conjugate induced more apoptosis and necrosis than NuBCP-9-R8 conjugate at 10 μM.

DISCUSSION

Oligoarginines, as a type of CPP, have been commonly utilized for intracellular delivery of therapeutic peptides because of the simple synthesis procedure and high uptake efficiency of conjugates.[11] NuBCP-9, a Bcl-2 targeting proapoptotic peptide, has been proven to have synergy with R8, and the resultant conjugate exhibited enhanced uptake efficiency while also inducing a degree of non-specific membrane disruption.[15] Although such an enhanced uptake effect has been seen with other CPPs after reverting the hydrophobicity of other cargo peptide, the degree of enhancement has generally relied on the intrinsic uptake efficiency of the CPPs used.[12] In the case
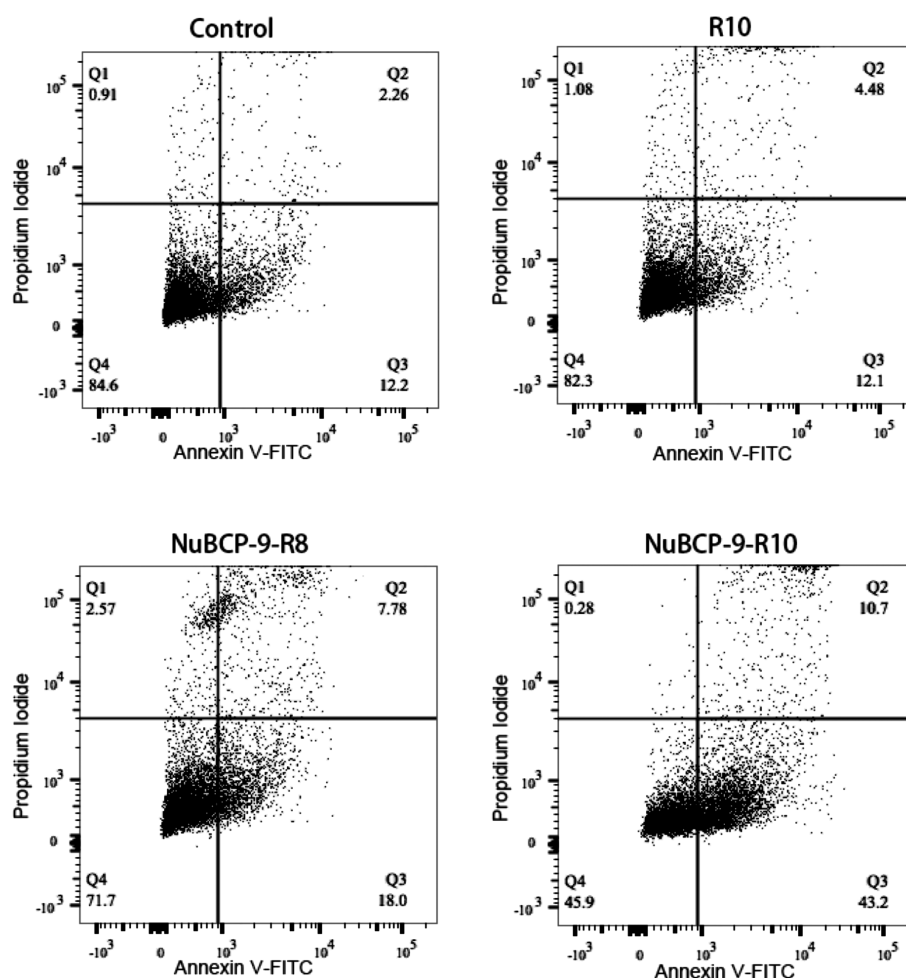
Fig. 6.   Apoptosis Levels Induced by Peptides

After a 2 h incubation with 10μM unlabeled NuBCP-9-R8, NuBCP-9-R10 conjugates and R10 and then a 22 h incubation in their absence, apoptosis was induced in MDA-MB-231 cells. The level of apoptosis was determined from Annexin-V/PI staining observed by flow cytometry. 10000 counts were taken for each sample.

of oligoarginines, uptake efficiency has been shown to be dependent on the number of arginines present in the oligomer.[14] Therefore, Rn of different lengths may perform differently in terms of uptake efficiency and non-specific cytotoxicity following conjugation with NuBCP-9.

We first evaluated the uptake efficiency and cellular distribution of Rn before and after conjugation with NuBCP-9, to investigate how NuBCP-9 influences the uptake behavior of Rn of different lengths. Without conjugating of Rn, NuBCP-9 was difficult to be delivered into cells, while NuBCP-9-Rn conjugates showed significant uptake (Figs. 1A, B), it suggests that Rn ($n=8$, 10, 12, 14) may be the vectors to induce the uptake of NuBCP-9. The uptake levels of unconjugated Rn and NuBCP-9-Rn conjugates at concentrations of 2μM were only slightly different (Fig. 1B), but uptake of NuBCP-9-Rn conjugates at concentrations of 10μM was significantly elevated compared to uptake of Rn administered at the same concentration (Fig. 1C). The uptake behavior of cationic CPPs, including oligoarginines, has been shown to demonstrate differing behavior above and below a concentration threshold in previous studies as well.[21,22] We showed that the uptake level of R8 exhibited a mild increase according to a cumulative gradient of treatment concentration, but the uptake efficiency of NuBCP-9-R8 conjugate increased dramatically after reaching a 4μM concentration threshold (Fig. 1A). This suggests

that a threshold concentration of peptides may be critical for promoting internalization of Rn following conjugation with NuBCP-9, which could explain the differing performance of NuBCP-9-Rn conjugates at concentrations of 2 and 10μM. The most effective length for intracellular delivery of NuBCP-9 was 10 arginines in R10, although unconjugated R12 showed higher uptake efficiency at a concentration of 10μM (Fig. 1C). Many studies have similarly shown that a longer oligoarginines has a higher uptake capacity with a variety of peptide cargo.[21,24,25]

With respect to cellular distribution of the internalized peptides, CLSM (Figs. 1D, E) yielded results similar to those obtained by flow cytometry (Figs. 1B, C). Unconjugated R8 was distributed into a punctate structure, whereas cytosolic labelling was observed in cells treated with NuBCP-9-R8 conjugate at 10μM (Fig. 1E). It has been reported that R12 shows diffuse cytosolic labelling when its concentration crosses the threshold level.[21] The differing cellular distribution between Rn and NuBCP-9-Rn conjugates administered at concentrations of 10μM suggests that NuBCP-9 may reduce threshold concentration for effective cytosolic distribution. Overall, NuBCP-9-Rn conjugates may promote cellular uptake at a relatively high concentration.

Many studies have shown that hydrophobic modification increases the uptake efficiency of CPPs.[12,13] Although previous

studies considered the N-terminal phenylalanine of NuBCP-9 important in the enhanced uptake of R8, there is little information about the influence of the C-terminal leucine.[15] In our study, we the replaced C-terminal leucine of NuBCP-9-R8 (FSRSLHSLL-R8) with alanine (FA-R8). We found that this Leu-Ala replacement led to a significant decrease in R8 uptake, and that a subsequent replacement of the N-terminal phenylalanine with alanine reduced it further still. Our results showed that the N-terminal phenylalanine plays a greater role in uptake enhancement than the C-terminal leucine (Fig. 3). The aromatic side chain may endow phenylalanine with higher hydrophobicity, and consequently greater ability to enhance uptake of R8 in a NuBCP-9-R8 conjugate, than the aliphatic side chain of leucine.[26,27] Our work suggests that not only phenylalanine but also leucine in the amino acid sequence of NuBCP-9 makes a contribution to the enhanced uptake of Rn.

For investigating whether the enhanced uptake efficiency of NuBCP-9-Rn conjugates is related to a change in uptake pathway being used, we analyzed the uptake behaviors of Rn and NuBCP-9-Rn conjugates using specific uptake inhibitors. Inhibitors of endocytosis, clathrin-mediated endocytosis,[28,29] caveolae-mediated endocytosis[29] and macropinocytosis,[23,29,30] have been proven to partly influence Rn uptake. The uptake behavior of both Rn and NuBCP-9-Rn conjugates were suppressed following treatment with chlorpromazine or EIPA (Figs. 2A, B, Fig. S2). In agreement with these findings, Kawaguchi *et al.* reported that the uptake of R8 was mediated by both clathrin-mediated endocytosis and macropinocytosis, but not caveolae-mediated endocytosis.[28] In addition to these endocytosis pathways, direct transduction of oligoarginines has also been reported.[30,31] In the presence of chlorpromazine or EIPA, we clearly observed nuclear staining (Figs. 2C, D, Fig. S3) in MDA-MB-231 cells treated with Rn or NuBCP-9-Rn conjugates, suggesting nuclear transport of peptides unmediated by endocytosis.[30,31] These observations, in agreement with previous studies, indicate that the uptake of Rn and NuBCP-9-Rn conjugates are partly regulated by clathrin-mediated endocytosis and macropinocytosis, and partly by direct transduction.

Effective uptake is important to ensure cellular efficacy of the therapeutic entity, but the administered drug or molecules must not exhibit high non-specific cytotoxicity. We aimed to research the correlation between cellular uptake level and intracellular cytotoxicity caused by NuBCP-9 conjugation Rn of different lengths. Up to a concentration of $15\,\mu$M, NuBCP-9, NuBCP-9-R4 and NuBCP-9-R6 conjugates induced slight toxicity, while NuBCP-9 with longer Rn ($n=8, 10, 12, 14$) resulted in greater cytotoxicity at the same dose (Fig. 4A). Without conjugation, only R14 led to severe cellular toxicity at $15\,\mu$M (Fig. 4B), suggesting that NuBCP-9 is the source of the differing cytotoxicity between conjugated and unconjugated Rn. NuBCP-9-R14 conjugate showed the highest cytotoxicity in MDA-MB-231 cells. However, NuBCP-9-R10 conjugate exhibited the most effective uptake as determined by flow cytometry (Fig. 1C). This limited correlation between uptake level and cytotoxicity suggests that the Bcl-2-based mechanism of internalized peptides was not the only source of NuBCP-9-Rn conjugates-induced cytotoxicity. The non-specific cytotoxicity from relatively long Rn was caused by membrane disruption resulting from the high density positive charge formed around the cell membrane. This can also be seen in studies where R16

exhibits higher non-specific cytotoxicity and uptake efficiency than R8.[14,22,23] Furthermore, a non-specific necrotic effect induced by NuBCP-9-R8 conjugate has also been demonstrated in previous studies.[15] Thus, it is assumed that the poor correlation between uptake level and cytotoxicity is the result of necrosis unrelated to Bcl-2. Therefore, to evaluate non-specific cytotoxicity, we chose to determine the level of membrane disruption caused by Rn and NuBCP-9-Rn conjugates. NuBCP-9 conjugated with R12 and R14 induced more LDH release at a concentration of $10\,\mu$M, and were therefore deemed to cause intolerable non-specific cytotoxicity. However, without NuBCP-9 conjugation, even R14 had only negligible effects on membrane integrity, as shown in Fig. 5. These results suggest NuBCP-9 aggravates the membrane perturbance caused by R12 and R14. For this reason, R12 and R14 may not be suitable choices for conjugation with NuBCP-9 in this context.

On a related point, the decreasing uptake levels of NuBCP-9-R12 and NuBCP-9-R14 conjugates at concentrations of $10\,\mu$M when compared to that of the NuBCP-9-R10 conjugate (Fig. 1C) might be explained by non-specific cytotoxicity resulting in poor membrane integrity, which in turn makes it impossible for the internalized peptides to remain within the cells long enough to exert their full effects.

Finally, NuBCP-9 has been proven to act through Bcl-2 to induce apoptosis.[6] We detected the level of apoptosis induced by NuBCP-R8 and NuBCP-9-R10 conjugates. Just as in Fig. 1C, Fig. 6 shows that NuBCP-9-R10 conjugate induced a higher level of apoptosis than NuBCP-9-R8 conjugate, which might reflect the correlation between uptake capacity and intracellular activity. Nakase *et al.* showed that the level of apoptosis induced by pro-apoptotic domain peptide (PAD)-Rn conjugates was related to intracellular uptake level.[23] Taking this into consideration, the higher level of apoptosis induced by NuBCP-9-R10 conjugate may be related to its relatively high cellular uptake, which can lead to more specific interaction between NuBCP-9 and Bcl-2 in the cells.

In conclusion, we analyzed the uptake characteristics and cytotoxicity of Rn and NuBCP-9-Rn conjugates. NuBCP-9 conjugated with Rn enhanced cellular uptake, which involved clathrin-mediate endocytosis and macropinocytosis–uptake pathways that were not changed from those used by unconjugated Rn. The cytotoxicity study showed that NuBCP-9-R12 and NuBCP-9-R14 conjugates magnified non-specific cytotoxicity. As a consequence, we found that NuBCP-9-R10 conjugate is the most suitable compound for pro-apoptotic therapeutic application of NuBCP-9 because it possessed the highest uptake efficiency and induced high levels of apoptosis in MDA-MB-231 cells. The information in this study will be valuable in the design of a pro-apoptotic peptide conjugated with oligoarginines for anti-cancer therapy.

Conflict of Interest The authors declare no conflict of interest.

Supplementary Materials The online version of this article contains supplementary materials.

REFERENCES

1) Torchilin V. Tumor delivery of macromolecular drugs based on the EPR effect. *Adv. Drug Deliv. Rev.*, **63**, 131–135 (2011).

2) Ellerby HM, Arap W, Ellerby LM, Kain R, Andrusiak R, Del Rio G, Krajewski S, Lombardo CR, Rao R, Ruoslahti E. Anti-cancer activity of targeted pro-apoptotic peptides. *Nat. Med.*, **5**, 1032–1038 (1999).

3) Raina D, Kosugi M, Ahmad R, Panchamoorthy G, Rajabi H, Alam M, Shimamura T, Shapiro GI, Supko J, Kharbanda S, Kufe D. Dependence on the MUC1-C oncoprotein in non-small cell lung cancer cells. *Mol. Cancer Ther.*, **10**, 806–816 (2011).

4) Cory S, Roberts AW, Colman PM, Adams JM. Targeting BCL-2-like proteins to kill cancer cells. *Trends in Cancer*, **2**, 443–460 (2016).

5) Beekman AM, Howell LA. Small-molecule and peptide inhibitors of the prosurvival protein Mcl-1. *ChemMedChem*, **11**, 802–813 (2016).

6) Kolluri SK, Zhu X, Zhou X, Lin B, Chen Y, Sun K, Tian X, Town J, Cao X, Lin F, Zhai D, Kitada S, Luciano F, O'Donnell E, Cao Y, He F, Lin J, Reed JC, Satterthwait AC, Zhang XK. A short Nur77-derived peptide converts Bcl-2 from a protector to a killer. *Cancer Cell*, **14**, 285–298 (2008).

7) Alves ID, Carré M, Montero M-P, Castano S, Lecomte S, Marquant R, Lecorché P, Burlina F, Schatz C, Sagan S, Chassaing G, Braguer D, Lavielle S. A proapoptotic peptide conjugated to penetratin selectively inhibits tumor cell growth. *Biochim. Biophys. Acta*, **1838**, 2087–2098 (2014).

8) Kim D, Lee I-H, Kim S, Choi M, Kim H, Ahn S, Saw PE, Jeon H, Lee Y, Jon S. A specific STAT3-binding peptide exerts antiproliferative effects and antitumor activity by inhibiting STAT3 phosphorylation and signaling. *Cancer Res.*, **74**, 2144–2151 (2014).

9) Nishimura K, Fumoto S, Fuchigami Y, Hagimori M, Maruyama K, Kawakami S. Effective intraperitoneal gene transfection system using nanobubbles and ultrasound irradiation. *Drug Deliv.*, **24**, 737–744 (2017).

10) Kilpeläinen M, Riikonen J, Vlasova M, Huotari A, Lehto V, Salonen J, Herzig K, Järvinen K. *In vivo* delivery of a peptide, ghrelin antagonist, with mesoporous silicon microparticles. *J. Control. Release*, **137**, 166–170 (2009).

11) Heitz F, Morris MC, Divita G. Twenty years of cell-penetrating peptides: from molecular mechanisms to therapeutics. *Br. J. Pharmacol.*, **157**, 195–206 (2009).

12) Sayers EJ, Cleal K, Eissa NG, Watson P, Jones AT. Distal phenylalanine modification for enhancing cellular delivery of fluorophores, proteins and quantum dots by cell penetrating peptides. *J. Control. Release*, **195**, 55–62 (2014).

13) Takayama K, Nakase I, Michiue H, Takeuchi T, Tomizawa K, Matsui H, Futaki S. Enhanced intracellular delivery using arginine-rich peptides by the addition of penetration accelerating sequences (Pas). *J. Control. Release*, **138**, 128–133 (2009).

14) Mitchell DJ, Steinman L, Kim D, Fathman C, Rothbard J. Polyarginine enters cells more efficiently than other polycationic homopolymers. *Chem. Biol. Drug Des.*, **56**, 318–325 (2000).

15) Watkins CL, Sayers EJ, Allender C, Barrow D, Fegan C, Brennan P, Jones AT. Co-operative membrane disruption between cell-penetrating peptide and cargo: implications for the therapeutic use of the Bcl-2 converter peptide D-NuBCP-9-r8. *Mol. Ther.*, **19**, 2124–2132 (2011).

16) Jones SW, Christison R, Bundell K, Voyce CJ, Brockbank S, Newham P, Lindsay MA. Characterisation of cell-penetrating peptide-mediated peptide delivery. *Br. J. Pharmacol.*, **145**, 1093–1102 (2005).

17) Arisan ED, Kutuk O, Tezil T, Bodur C, Telci D, Basaga H. Small inhibitor of Bcl-2, HA14-1, selectively enhanced the apoptotic effect of cisplatin by modulating Bcl-2 family members in MDA-MB-231 breast cancer cells. *Breast Cancer Res. Treat.*, **119**, 271–281 (2010).

18) Zapata JM, Krajewska M, Krajewski S, Huang R-P, Takayama S, Wang H-G, Adamson E, Reed JC. Expression of multiple apoptosis-regulatory genes in human breast cancer cell lines and primary tumors. *Breast Cancer Res. Treat.*, **47**, 129–140 (1998).

19) Suga T, Fuchigami Y, Hagimori M, Kawakami S. Ligand peptide-grafted PEGylated liposomes using HER2 targeted peptide-lipid derivatives for targeted delivery in breast cancer cells: the effect of serine-glycine repeated peptides as a spacer. *Int. J. Pharm.*, **521**, 361–364 (2017).

20) Un K, Kawakami S, Suzuki R, Maruyama K, Yamashita F, Hashida M. Development of an ultrasound-responsive and mannose-modified gene carrier for DNA vaccine therapy. *Biomaterials*, **31**, 7813–7826 (2010).

21) Kosuge M, Takeuchi T, Nakase I, Jones AT, Futaki S. Cellular internalization and distribution of arginine-rich peptides as a function of extracellular peptide concentration, serum, and plasma membrane associated proteoglycans. *Bioconjug. Chem.*, **19**, 656–664 (2008).

22) Tünnemann G, Ter-Avetisyan G, Martin RM, Stöckl M, Herrmann A, Cardoso MC. Live-cell analysis of cell penetration ability and toxicity of oligo-arginines. *J. Pept. Sci.*, **14**, 469–476 (2008).

23) Nakase I, Niwa M, Takeuchi T, Sonomura K, Kawabata N, Koike Y, Takehashi M, Tanaka S, Ueda K, Simpson JC, Jones AT, Sugiura Y, Futaki S. Cellular uptake of arginine-rich peptides: roles for macropinocytosis and actin rearrangement. *Mol. Ther.*, **10**, 1011–1022 (2004).

24) Furuhata M, Kawakami H, Toma K, Hattori Y, Maitani Y. Design, synthesis and gene delivery efficiency of novel oligo-arginine-linked PEG-lipids: Effect of oligo-arginine length. *Int. J. Pharm.*, **316**, 109–116 (2006).

25) Takayama K, Tadokoro A, Pujals S, Nakase I, Giralt E, Futaki S. Novel system to achieve one-pot modification of cargo molecules with oligoarginine vectors for intracellular delivery. *Bioconjug. Chem.*, **20**, 249–257 (2009).

26) Wimley WC, White SH. Experimentally determined hydrophobicity scale for proteins at membrane interfaces. *Nat. Struct. Mol. Biol.*, **3**, 842–848 (1996).

27) Matsubara T, Iida M, Tsumuraya T, Fujii I, Sato T. Selection of a carbohydrate-binding domain with a helix–loop–helix structure. *Biochemistry*, **47**, 6745–6751 (2008).

28) Kawaguchi Y, Takeuchi T, Kuwata K, Chiba J, Hatanaka Y, Nakase I, Futaki S. Syndecan-4 is a receptor for clathrin-mediated endocytosis of arginine-rich cell-penetrating peptides. *Bioconjug. Chem.*, **27**, 1119–1130 (2016).

29) Duchardt F, Fotin-Mleczek M, Schwarz H, Fischer R, Brock R. A comprehensive model for the cellular uptake of cationic cell-penetrating peptides. *Traffic*, **8**, 848–866 (2007).

30) Zaro JL, Shen W-C. Evidence that membrane transduction of oligoarginine does not require vesicle formation. *Exp. Cell Res.*, **307**, 164–173 (2005).

31) Zaro JL, Vekich JE, Tran T, Shen W-C. Nuclear localization of cell-penetrating peptides is dependent on endocytosis rather than cytosolic delivery in CHO cells. *Mol. Pharm.*, **6**, 337–344 (2009).